RSC Advances

REVIEW

View Article Online
View Journal | View Issue

Cite this: *RSC Adv.*, 2023, **13**, 9466

Research progress of catalysts for aldol condensation of biomass based compounds

Xing Zhang,[a] YanQing Li,[a] Chi Qian,[a] Ling An,[a] Wei Wang, *[a] XiuFeng Li,[b] XianZhao Shao [a] and Zhizhou Li[a]

Research progress of catalysts of the aldol condensation reaction of biomass based compounds is summarized for the synthesis of liquid fuel precursors and chemicals. In summary, an acidic catalyst, alkaline catalyst, acid–base amphoteric catalyst, ionic liquid and other catalysts can catalyze the aldol condensation reaction. The aldol condensation reaction catalyzed by an acid catalyst has the problems of low conversion and low yield. The basic catalyst catalyzes the aldol condensation reaction with high conversion and yield, but the existence of liquid alkali is difficult to separate from the product. The reaction temperature needed for oxide and hydrotalcite alkali is relatively high. The basic resin has good catalytic activity and at a low reaction temperature, and is easy to separate from the target product. Acid–base amphoteric catalysts have received extensive attention from researchers for their excellent activity and selectivity. Ionic liquid is a new type of material, which can also be used for the aldol condensation reaction. In the future application of aldol condensation, the development of strong alkaline resin is a good research direction.

Received 10th February 2023
Accepted 17th March 2023

DOI: 10.1039/d3ra00906h

rsc.li/rsc-advances

Introduction

Fossil fuel is one of the main energy sources in the world. For a long time in the future, fossil fuels will still be used by humans as the main energy source. However, with the increasing attention on renewable energy and sustainable development, the catalytic conversion of renewable, cheap and inedible lignocellulose into renewable fuels[1,2] has attracted the attention of many scholars. The carbon number of compounds in biomass-based materials is generally C_5–C_6, which is much lower than the carbon number requirements of diesel and aviation kerosene. Therefore, it is necessary to increase the carbon chain of biomass platform compounds to increase their use value. Commonly, carbon–carbon coupling (C–C) reactions (aldol condensation,[3,4] hydroxyl alkylation/alkylation,[5] benzoic acid condensation,[6] Robinson cyclization reaction[7] and Diels–Alder reaction,[8,9] *etc.*) are used to obtain the desired product, which has important use value for human life.

We focus on the aldol condensation reaction because today's biomass platform compounds are catalytically converted into renewable liquid fuels[10] and under mild conditions,[11,12] with a reaction temperature less than 453 K. Simultaneously, new C–C bonds are formed by reducing the O/C ratio, and the carbon chain is increased, over acidic or alkaline catalysts. Moreover, β-hydroxyaldehydes or ketones, or α,β-unsaturated aldehydes and ketones can also be generated.

The essence of aldol condensation is nucleophilic addition reaction. If different substrates have α-H, they can undergo self-condensation and cross-reaction, which will complicate the product and reduce the selectivity of the target product. Therefore, in industrial production, in order to prevent the formation of by-products, basically the choice is cross-reaction. However, sometimes the reaction substrate cannot be changed at will and it is worth noting that high yields of aldol condensation of any specific product are difficult to achieve because many self-condensation and cross-condensation reactions usually have similar rates.[13] In this situation, where we requires a special catalyst to catalyze the aldol condensation reaction to enhance the selectivity of the target product. This paper reviews the application of catalysts commonly used in aldol condensation reaction in recent years, including acidic catalyst, alkaline catalyst, acid–base amphoteric catalyst, ionic liquid and other catalyst.

Acidic catalyst

Acidic catalysts include lewis acids, acid resins, acid molecular sieves, acid oxides and other solid acids.

At present, there are many examples of catalytic aldol condensation using acidic materials, but the products obtained after catalytic aldol condensation reaction are often used as raw materials for the next reaction, so there are technical problems such as purification and separation.

[a]*Shaanxi Key Laboratory of Catalysis, School of Chemistry and Environment Science, Shaanxi University of Technology, No. 1 Dong Yi Huan Road, Hanzhong 723001, China. E-mail: wangwei@snut.edu.cn*

[b]*Hanzhong Institute of Agricultural Science, No. 356, Dongta North Road, Hanzhong, 723000, China. E-mail: Lixiufengmm@126.com*

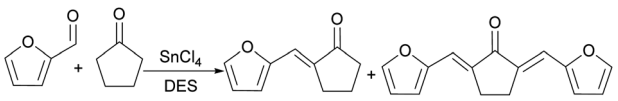

Fig. 1 Condensation reaction of furfural and cyclopentanone.

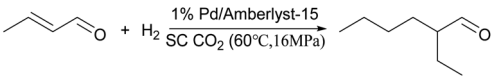

Fig. 2 Preparation of 2-ethyl hexanal by hydrogenation condensation of crotonaldehyde.

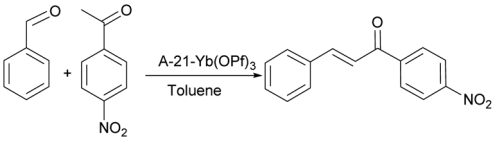

Fig. 3 Condensation reaction of benzaldehyde with *p*-nitroacetophenone.

Lewis acids

Yunyun Liu[14] used a eutectic solution (EDS) composed of choline chloride (ChCl) (hydrogen bond acceptor)–formic acid (Fa) (hydrogen bond donor)–$SnCl_4 \cdot 5H_2O$ (Lewis acid) to catalyze the aldol condensation reaction between furfural and cyclopentanone. The reaction route is shown in Fig. 1. Compared with ionic liquids, co-crystal solvents have the characteristics of low cost and biodegradability, and are green solvents. When the temperature is 100 °C, the reaction time is 120 min, the content of $SnCl_4 \cdot 5H_2O$ in the cocrystal solution is 2 mmol/5 g-EDS, the molar ratio of Fa/ChCl is 12 : 1, the molar ratio of furfural : cyclopentanone is 1 : 6, the conversion of furfural is 99.81%, the total yield is 92.03%, the yields of C_{10} and C_{15} are 47.55% and 44.48% respectively. If the reaction continues to heat up, the yield will decrease. The reason may be that the boiling point of formic acid is 100.8 °C, and the heating will cause its volatilization, which will cause the hydrogen bond between Fa and ChCl to be destroyed, which will lead to the imbalance of the eutectic solution system. It is worth mentioning that the yield is better than Wang Wei's.[15] Wang Wei used a solid acid catalyst, namely Nafion resin, under solvent-free conditions, to obtain an intermediate yield of 61.55%. Details are detailed below in acid resin.

Acidic resin

Wei Wang[15] used a series of solid acid catalysts, Nafion, Amberlyst-15, Amberlyst 36, H-USY, ZSM-5, H-β, *etc.*, to catalyze the aldol condensation reaction between cyclopentanone and furfural under solvent-free conditions. Compared with acidic molecular sieves, Nafion, Amberlyst 15, Amberlyst 36 and other resins have higher C_{10} and C_{15} yields, which are 23.77% and 37.48%, respectively. This may be due to the higher acid strength of the acid resin itself. The first step of the reaction requires protonated cyclopentanone to initiate the reaction. When C_{10} is formed, the subsequent reaction step, that is, the formation of C_{15} and C_{10}, also requires protonated cyclopentanone to promote the reaction. Therefore, the extent of the reaction can be determined by whether the proton can be protonated cyclopentanone.

Tsunetake Seki[16] used a bifunctional acidic palladium resin as a catalyst, Pd/Amberlyst-15, and crotonaldehyde as a raw material, supercritical CO_2 as a reaction medium, the direct synthesis of 2-ethyl hexanal, the reaction route is shown in Fig. 2. When the carrier was not acidic, 1% Pd/C was used to catalyze crotonaldehyde, 2-ethyl hexanal was not detected in the catalytic product. When 1%-Pd/Amberlyst-15 was used to catalyze crotonaldehyde, the selectivity of 2-ethyl hexanal was up to 67%. Transition metals can promote hydrogenation, but cannot promote the aldol condensation reaction of butyraldehyde itself. Therefore, the focus of one-step conversion from crotonaldehyde to 2-ethyl hexanal is that the strength of the catalyst's acidity and alkalinity promotes the aldol condensation reaction in this reaction.

Wen Bin Yi[17] used Amberlyst-21 as the carrier and loaded $Yb(OTf)_3$ to prepare a perfluorosulfonic acid catalyst. Because of its structural characteristics, the catalyst can be in the fluorine-free solvent system. In the direction of acylation, esterification, nitrification, aldol condensation, *etc.*, all have good catalytic performance. The aldol condensation reaction between various aldehydes and aromatic ketones was investigated. Benzaldehyde and acetophenone were used as structural units, para substituents were changed, the amount of feed was 12 mmol (aldehyde) : 20 mmol (ketone), toluene was used as solvent, the amount of catalyst was 0.25 mol%, and condensation reflux was used during the reaction. When the aldehyde and ketone substituents are hydrogen and nitro respectively, that is, the reaction is benzaldehyde and *p*-nitroacetophenone. The reaction route is shown in Fig. 3. When the reaction conditions are as above, the highest yield is 95%.

Acidic molecular sieve

Oleg Kikhtyanin,[18] for the first time, applied different types of acidic molecular sieves, such as H-ZSM-5, H-BEA, H-USY, to the aldol condensation reaction between furfural and acetone. The reaction route is shown in Fig. 4. When the reaction temperature is 100 °C and the reaction time is 2 h, the catalytic performance of H-BEA is the best and the yield of C_8 is 30.6%. The catalytic effect of H-BEA is better than other molecular sieves, which is related to the structure and pore size of H-BEA molecular sieve. Al-Ani[19] used layered zeolites to catalyze the aldol condensation reaction between furfural and acetone. Layered zeolite molecular sieve, that is, intracrystalline mesopores are formed inside the macroporous molecular sieve to

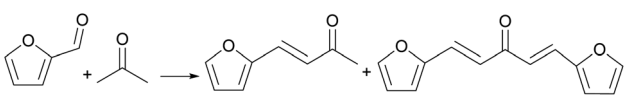

Fig. 4 Condensation reaction of furfural and acetone.

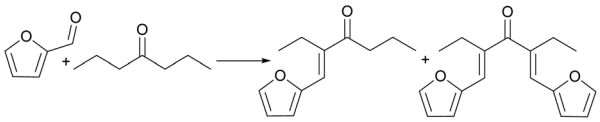

Fig. 5 Condensation reaction of furfural with 4-heptanone.

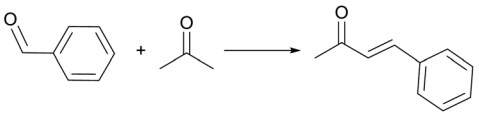

Fig. 7 Condensation reaction of benzaldehyde and acetone.

improve the availability of acidic sites in the molecular sieve. The active sites on the catalyst surface are easy to contact, but for the active sites inside the molecular sieve, it depends on the size of the guest molecule.[20]

For this reaction, the increased availability of acidic sites can promote the conversion of furfural, but also promote the self-condensation reaction of acetone, resulting in a decrease in the selectivity of the target product. Continuously increasing the acidity can increase the conversion rate, but it will cause unnecessary trouble in the subsequent purification steps.

Acidic oxide

Jing[21] used Nb_2O_5 to catalyze the reaction of furfural and 4-heptanone. The reaction route is shown in Fig. 5. When the molar ratio of furfural to 4-heptanone is 1 : 4, the amount of catalyst is 0.15 mol%, the reaction time is 4 hours and the reaction temperature is 130 °C, the conversion of furfural is 82.2%, which is more than twice as high as that of other catalysts such as MgO, CaO and ZrO_2. Compared to other catalysts, Nb_2O_5 can effectively activate the C=O bond in the carbonyl group to form an enol intermediate and also promote the cleavage of the C–O bond.[22]

Amarasekara[23] used SiO_2–SO_3H to catalyze the self-dipolycondensation of levulinic acid. The reaction route is shown in Fig. 6. When the reaction temperature reaches 130 °C, the highest dimer yield is 56%, and there are five dimer products in this reaction.

Lewis[24] used Hf-β, Sn-β, Zr-β zeolite molecular sieves to catalyze the reaction of benzaldehyde and acetone. The reaction route is shown in Fig. 7. Lewis acid zeolite is a special catalyst for activating carbonyl-containing molecules.[25–27] When the metal content ratio of aldehyde/ketone/zeolite molecular sieve is 150 : 50 : 1, the reaction temperature is 90 °C, and the reaction time is 5 h, the aldehyde conversion in the Hf-/Zr-β zeolite molecular sieve catalytic reaction is 90% and 97%, respectively, which is determined by the polarizability of the metal atom in the active center of the zeolite molecular sieve and the Brønsted base associated with the oxygen atom.[28] Zr and Hf belong to the same group of elements and have the same arrangement of electrons outside the nucleus, so they have similar catalytic properties. The outer electronic configuration of Sn is quite different, with σ* electrons.[29,30] In early years, Wen Zhi Li[31,32] used Lewis acidic zeolites containing Sn-MFI and Sn-beta skeleton structures to catalyze the aldol condensation reaction between furfural and acetone for the production of liquid fuel intermediates. The activity of Sn-beta is better than that of Sn-MFI, because the pore size of Sn-beta is larger than that of Sn-MFI, but the high activity and selectivity are reduced.

Now the research group, potassium supported on Lewis acid zeolite Sn-MFI, used it to catalyze the aldol condensation reaction between furfural and acetone. When the molar ratio of furfural and acetone is 1 : 10, the reaction temperature is 160 °C, the amount of catalyst is 0.1 mol%, the content of potassium is 5%, and the reaction time is 1 h, the maximum conversion rate of furfural is 100%. As the potassium content decreases or increases, the conversion rate gradually decreases. This is due to the interaction between K and Sn. When the metal is completely connected or interacted with the zeolite molecular sieve, that is, only Si–O–M, the catalytic performance is much weaker than that of partially connected, that is, M−OH groups.

Tingting Yan studied Lewis acid Y/β zeolite, in the process of ethanol catalytic conversion of butadiene, the catalyst in this reaction aldol condensation reaction, the effect is remarkable, the reaction mechanism is shown in Fig. 8.[33,34] The reaction is due to the limitation of the zeolite's own pores,[33] which can increase the probability of reactants reacting at the active site to generate the target product. In order to better understand the effect of zeolite itself and carrier on the catalytic performance of aldehyde condensation, Tingting Yan[35] studied the effect of rare earth cations and β zeolite on the catalytic performance of aldehyde condensation on the original basis, and found that in the self-condensation reaction of acetaldehyde, the dehydration of aldehydes and alcohols is the rate-determining step,[36,37] Y–OH is the preferred site for the aldol condensation reaction, these sites become more stable due to the presence of β zeolite carrier. The formation of hydrogen bonds between O in the Y–OH and H in the transition state plays an important role in the stability of the transition state of the aldol dimer and the reduction of the dehydration energy barrier. The catalyst, namely zeolite-stabilized Lewis acid rare earth cations, opens up a new way for unconventional rare earth catalysts.

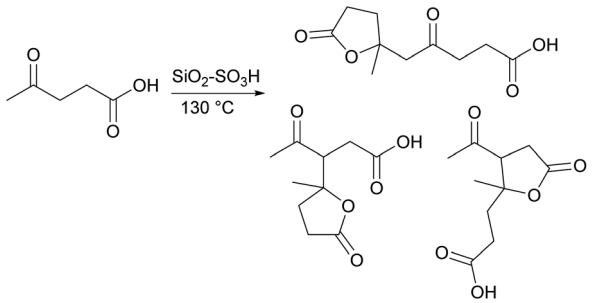

Fig. 6 Self-dipolycondensation of levulinic acid.

Other solid acids

M. Yu Talanova[38] used tetraphenylmethane as a mesoporous aromatic skeleton to prepare a tetraphenylmethane-SO_3H

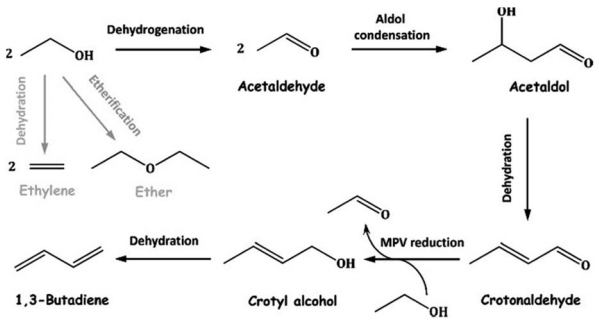

Fig. 8 Dehydration and condensation reaction route of ethanol.

catalyst for the aldol condensation reaction between furfural and acetone. In order to ensure the liquid phase reaction conditions, 1.0 MPa inert gas was added to each reaction. When the molar ratio of furfural to acetone was 1 : 10, the reaction temperature was 130 °C, and the sulfonate content was 2.5 mol%, the highest yield was obtained, about 25%. Composed of aromatic ring mesoporous aromatic skeleton, has a high specific surface area, acid and alkali resistance, and the structure and surface can be modified, such as cross-coupling, alkylation, reductive amination catalyst carrier,[39–43] so broad prospects in related fields. In addition to aromatic hydrocarbons as the skeleton, the skeleton can also be replaced to reduce the overall catalyst size.

Haofei Gao[44] used titanium sulfate nanofibers (STNFs) as catalysts to catalyze the aldol condensation reaction between vanillin and cyclohexanone. The reaction route is shown in Fig. 9. Specifically, STNFs were prepared by using TiO_2 anatase crystal as the skeleton, followed by sulfonation and other steps. When the reaction temperature was 150 °C, the reaction time was 10 h, the amount of STNFs was 0.03 mol%, and the molar ratio of vanillin to cyclohexanone was 1 : 3, the maximum yield of 2-(4-hydroxy-3-methoxybenzylidene)cyclohexan-1-one was about 81%. Compared with other solid acids, such as Amberlyst-15 resin, Nafion resin, H–Y, H-β and H-ZSM-5 zeolites, the number of B acid sites in sulfonated STNFs is the largest and the acid strength is the highest. This may be the reason why the catalyst STNFs has the highest activity for the aldol condensation reaction between vanillin and cyclohexanone.

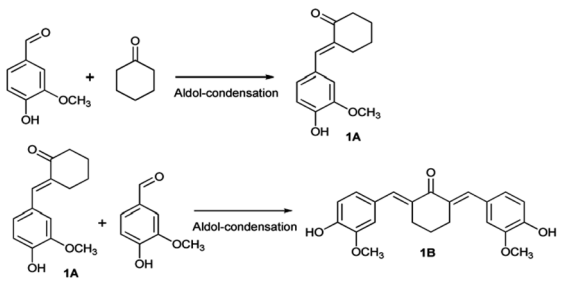

Fig. 9 The aldol condensation of vanillin and cyclohexanone.

Acidic catalytic mechanism

Under acid catalysis, the carbonyl group obtains a proton to form an enol structure after removing α-H, which forms a slightly negatively charged carbon system, while the protonated carbonyl group provides a slightly positively charged carbon system. The formation of new carbon–carbon bonds is completed by the nucleophilic addition of a partially negatively charged carbon to the activated carbonyl group.

In theory, the catalytic effect of homogeneous catalyst is better than that of heterogeneous catalyst, which is consistent with the results of our data listed. For example, compared with Nafion resin, the use of EDS can make the aldol condensation reaction yield between furfural and cyclopentanone higher, from 61.55% to 92.03%. However, homogeneous catalysts are difficult to separate, difficult to recycle, and will corrode equipment and other hidden dangers. However, if a reaction is in the laboratory research stage, the principal purpose is high conversion and yield. Separation is a secondary problem. If it comes to industrial use, the heterogeneous catalyst may be the first choice. Because the benefits of high catalysis, high conversion and high yield brought by homogeneous catalysis may not cover the cost of separation, purification and maintenance equipment. Therefore, in order to break through its existing boundaries, heterogeneous catalysis need to be continuously optimized by active site, from the original macromolecules to cluster groups to dozens of molecules, atoms, and even the final single atom catalysis. Based on this, the pursuit of high efficiency and low pollution emissions is the focus of future research.

Alkaline catalyst

Alkaline catalysts include liquid base, hydrotalcite-type solid base, alkaline resin, alkaline oxide, *etc.*

Generally speaking, alkaline catalysts are most used because they can directly attract α-H, form carbocations, attack carbon–oxygen double bonds, and form C–C coupling, but they are not resistant to CO_2 and H_2O.

Liquid alkali catalyst

Wei Wang[45] used NaOH as a catalyst to catalyze the self-condensation reaction of 3,3,5-trimethylcyclohexanone (TC) to generate 3,5,5-trimethyl-2-(3,3,5-trimethylcyclohexylidene) cyclohexanone (TCC). When the reaction temperature is 170 °C, the reaction time is 72 h, 0.143 mol of 2.50 mmol NaOH and 20 mL of *p*-xylene are used as solvents, TCC has a maximum carbon yield of about 76.4%. The self-condensation reaction has high temperature and long time span, which indicates that the reaction is not easy to carry out, and the aldol condensation reaction is reversible. Therefore, from the perspective of reaction equilibrium, the formation of water will inhibit the occurrence of aldol reaction. The Dean–Stark apparatus is usually connected to the reflux condenser and collector to ensure that the water generated by the reaction at the reflux temperature can be continuously discharged. Based on this, the

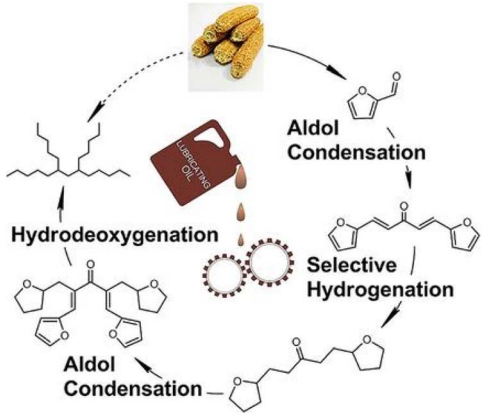

Fig. 10 Condensation reaction of furfural and acetone.

maximum carbon yield of TCC can be obtained under optimal conditions.

Yan Qin Wang[46] used a homogeneous alkaline catalyst, NaOH, to catalyze the aldol condensation reaction between furfural and acetone. First, furfural and acetone were used as substrates to synthesize the condensation product of C_{13}, and then selectively hydrogenated to produce C_{13} ketone. Finally, C_{13} ketone and furfural were subjected to secondary condensation to produce C_{23} condensation product. The reaction route is shown in Fig. 10.

In the condensation reaction, the amount of catalyst was 7.5 mol% NaOH, the reaction temperature was 40 °C, the reaction time was 5 h, and the final C_{13} yield was 97.4%. C_{13} can be dissolved in NaOH solution, which avoids the problem of subsequent separation and purification. After using Pt/γ-Al_2O_3 to catalyze hydrogenation to obtain C_{13} ketone, considering the solubility of organic matter, methanol was used as solvent to carry out subsequent condensation reaction. When the catalyst was 7.5 mol% NaOH, the reaction temperature was 50 °C, the reaction time was 20 h, and the furfural was excessive, that is, the furfural : C_{13} ketone was 8 : 1, the final C_{23} condensation product yield was 83.8%.

Iuliana Cota[47] used 1,5,7-triazabicyclo [4.4.0] dodec-5-ene (TBD) to catalyze the aldol condensation reaction between citral and methyl ethyl ketone. The reaction route is shown in Fig. 11. When the reaction time was 6 h and 9.84 mol% TBD, the conversion of methyl ethyl ketone was 99% and the selectivity of main product was 90%. While achieving excellent results, there are also corresponding measures for product purification and separation. A simple CO_2 fixation method was used. After the reaction, CO was bubbling for 30 min under normal temperature and pressure magnetic stirring, and the bubbling rate was 10 mL min^{-1}. White precipitate is obtained, filtered and heated to 130 °C in inert atmosphere to recover TBD.

Hydrotalcite-type solid base

At present, the cross-aldol reaction of furfural and ketone has been widely studied in the field of biomass catalytic conversion.[48–50] Jin Fan Yang[48] used Mg/Al atomic ratio of 5 : 1

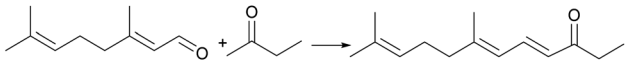

Fig. 11 Condensation reaction of citral and methyl ethyl ketone.

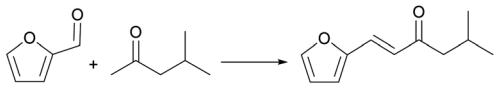

Fig. 12 Condensation reaction of furfural with methyl isobutyl ketone.

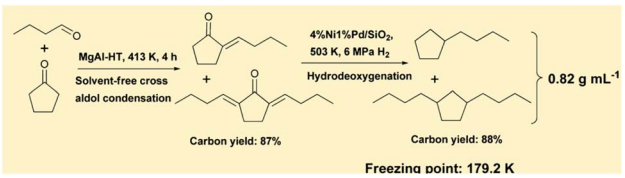

Fig. 13 Condensation reaction of cyclopentanone and butyraldehyde.

hydrotalcite catalyzed furfural and methyl isobutyl ketone (MIBK) reaction, the reaction route is shown in Fig. 12. The reaction substrate furfural/MIBK molar ratio was 1 : 2, 130 °C reaction 8 h, C_{11} oxide yield was 95%.

Laura Faba (**https://www.sciencedirect.com/science/article/pii/S0926337311005480?via%3Dihub#!**)[51] chose three solid base catalysts, Mg–Zr, Mg–Al, Ca–Zr, which have good activity and selectivity in other alkaline reactions, to catalyze the aldol condensation reaction between furfural and acetone. For the specific reaction, the catalytic performance of bimetallic solid base is better than that of monometallic solid base, which can be partly attributed to the synergistic effect between the two metals. Yue song Li[52] used Mg–Zr solid base catalyst for the transesterification of microalgae oil to biomass fuel. M. L. Rojas-Cervantes[53] used Mg–Zr to catalyze the brain-warping reaction between benzaldehyde and ethyl acetoacetate. Jin Fan Yang[54] used Mg–Al solid base catalyst to catalyze the aldol condensation reaction of cyclopentanone and butyraldehyde. The reaction route is shown in Fig. 13.

Mg–Al solid base catalyst was also used to catalyze self-condensation reaction of MIBK,[55] aldol condensation reaction of furfural and cyclohexanone.[56] The reaction route is shown in Fig. 14. Faba[51] used Mg–Zr as a catalyst to catalyze the aldol condensation reaction between furfural and acetone. When the molar ratio of furfural to acetone was 1 : 1, the Mg–Zr solid base had more strong basic sites than Mg–Al and Ca–Zr, so the Mg–Zr solid base had the highest reactivity and selectivity to C_{13}, and the final yield of C_{13} was about 60%.

Xue Lai Zhao[57] used NaOH-modified chitosan as a catalyst to catalyze the aldol condensation reaction between furfural and levulinic acid. The reaction route is shown in Fig. 15. Chitosan, chitin and cellulose have similar chemical structures. Chitosan is amino at C2 position, cellulose and chitin are hydroxyl and acetyl amino at C2 position respectively. These amino groups and furfural condensation can form Schiff bases, namely

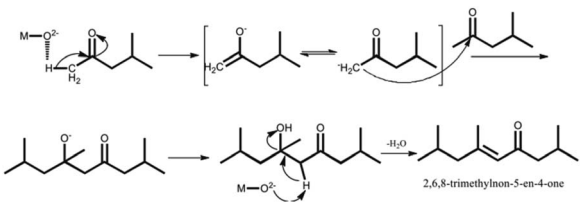

Fig. 14 Self-condensation reaction of MIBK.

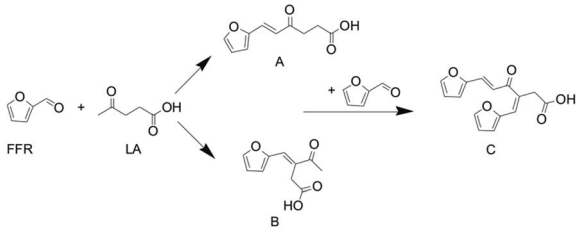

Fig. 15 Condensation reaction of furfural and levulinic acid.

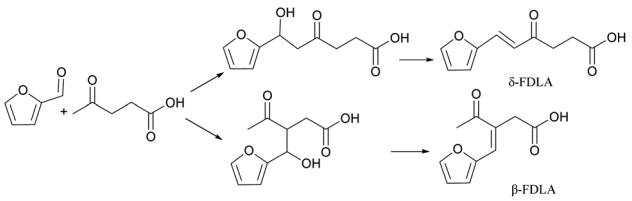

Fig. 16 Condensation reaction of furfural and levulinic acid.

imines or imine substitutes. The Schiff base then attacks the levulinic acid enol to form a Mannich base, namely a β-aminoketone derivative. Finally, the Mannich base[58,59] decomposed to obtain the target condensation product. That is, when the molar ratio of furfural to levulinic acid is 2 : 1, the catalyst is 0.25 mol%, the reaction time is 3 h, and the reaction temperature is 25 °C, the yields of C_{10} and C_{15} are 16.40% and 77.99%, respectively. This is the result of the synergistic effect between amino and sodium hydroxide. The yields of C_{10} and C_{15} directly catalyzed by sodium hydroxide are much lower than that of the above mentioned method.

Basic oxide

Fang Chen[60] used CaO and KF/Al_2O_3 as catalysts to catalyze the aldol condensation reaction between furfural and 3-pentanone. When the reaction temperature was 170 °C, the reaction time was 7 h, the molar ratio of furfural and 3-pentanone was 1 : 2, and the amount of catalyst was 0.25 mol%, the maximum yield of C_{10} was about 60%. Moreover, compared with KF/Al_2O_3 supported catalyst, CaO is the main component of lime, which is cheap, widely applicable and has low toxicity. On this basis, the research group expanded the substrate to explore whether furfural and nonanone yield would exceed 60% under the above optimal reaction conditions. The experimental data show that the longer the carbon chain, the greater the overall steric hindrance effect, which is unfavorable to the reaction, that is, the maximum yield is about 30%.

Boonrat Pholjaroen[61] used CaO as a catalyst for the aldol condensation reaction between furfural and MIBK. When the reaction temperature is 180 °C and the amount of CaO is 1 mol%, the molar ratio of furfural to MIBK is 3 : 100, which is mainly the MIBK phase product of the simulated xylose in the MIBK/water two-phase system. Under these conditions, the maximum yield of 1-(furan-2-yl)-5-methylhex-1-en-3-one (FMIBK) was 79.5%. The aldol condensation reaction has the characteristics of dehydration. CaO can react with water to form calcium hydroxide, which is another solid base, and the catalytic effect is completely different. This is due to the different number of strong base sites in the two solid bases, which are the active sites of MIBK and furfural.[48]

Guan Feng Liang[62] found that the aldol condensation reaction between levulinic acid and furfural catalyzed by Na_2CO_3 can usually obtain β or δ-furfurylidenelevulinic acids in a low yield in the aqueous phase, two monomer isomers,[63] the reaction route is shown in Fig. 16. However, this alkaline catalyst can simultaneously activate two α-hydrogens in levulinic acid, resulting in low product selectivity.

This is mainly due to the structural characteristics of levulinic acid. There are two kinds of α-H in levulinic acid. During polymerization, two kinds of enol structures can be formed, that is, C_1 and C_3 enol forms, and can be ringed after self-polymerization, so there will be five dimer products.

In order to improve the product selectivity, a series of alkaline catalysts were screened. When MgO was used and the molar ratio of levulinic acid/furfural was 1.5, the reaction was a typical alkaline catalytic mechanism, and the yield of δ-FDLA could reach 70.6%.

Yanting Liu[3] used MgO-p (prepared by precipitation method) as a catalyst for the intramolecular aldol condensation of 2,5-hexanedione (HD). When the reaction temperature is 180 °C, weight hourly space velocity (WHSV) = 1.7 g h^{-1}, hydrogen pressure is 0.1 MPa, and the molar ratio of hydrogen to HD is 52 : 1, 3-methylcyclopent-2-enone has a maximum carbon yield of about 98.3%. Compared with commercial MgO, the average particle size of MgO-p catalyst is 4 times smaller and BET is 6 times larger. There is no further condensation product, which may be explained by the conjugated structure of ketene.

Huber[64] reported that the activity of $MgO–ZrO_2$ increases with the increase of water content in the system during the aldol condensation reaction of furfural and acetone, which is due to the formation of surface hydroxyl groups on the exposed $MgO–ZrO_2$ surface. Faba[51] reported that acetone produced by fermentation of biomass ABE[65] has six α-H. In the condensation reaction, α-H is first extracted from acetone to obtain carbon anion, which then reacts with furfural to form aldehyde ketone, and finally dehydrated to form product.[10] In this reaction, in the process of carbanion induction, too strong or too weak alkali will lead to the destruction of the overall balance. Therefore, the moderate alkaline sites can make the aldol condensation reaction of furfural and acetone proceed smoothly, which also confirms the view of Huber *et al.*,[64] that is, the moderate surface hydroxyl basicity promotes the reaction. According to Huber

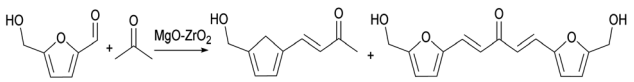

Fig. 17 Condensation of 5-hydroxymethylfurfural with acetone.

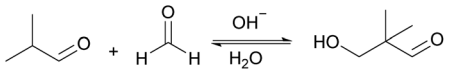

Fig. 18 Aldol condensation of isobutyraldehyde and formaldehyde.

et al.[64] and Liang *et al.*'s[62] point of view is that the active site is on Mg^{2+}–O^{2-} and surface hydroxyl. However, when ZnO was used as catalyst, the reaction time was 16 h and the reaction temperature was 95 °C, the reaction was acid catalytic mechanism, and the final yield of β-FDLA could reach 75.5%. These aldol reaction products are the precursors of the subsequent step hydrodeoxygenation, but these two steps can be combined into one step. Barrett[66] used Pd/MgO–ZrO_2 catalyst to catalyze the reaction of furfural or 5-hydroxymethylfurfural (HMF) with acetone. The reaction route is shown in Fig. 17. When the molar ratio of furfural to acetone was 1 : 1 and the reaction temperature was 80 °C, the yield of C_{13} was 85%. When the temperature rises again, the selectivity will not change but the carbon yield will gradually decrease, which is also the optimal solution to the balance between yield and carbon yield. When the molar ratio of HMF and acetone is 1 : 1, the reaction temperature is 50 °C, the reaction effect is the best, and the yield of C_{15} is 61%. It can be seen that the molar ratio and reaction temperature of the aldol reaction have a great influence on the selectivity and total yield of the reaction.

Alkaline resin

M. A. Tike[67] used a weakly basic anion exchange resin, Indion-860, to catalyze the aldol condensation reaction between formaldehyde and isobutyraldehyde. The reaction route is shown in Fig. 18. Before the reaction, Indion-860 is used to remove trace amounts of butyric acid and formic acid in the solution, which can reduce the formation of by-products such as acetals and hemiacetals. Due to the particularity of its structure, there is no α-H after cross acetylation, and Tishchenko reaction.[68–70] In order to prevent its self-condensation reaction, isopropanol was used as the reaction solvent. When the reaction temperature is 60 °C, the molar ratio of isobutyraldehyde and formaldehyde is 4 : 1, and the reaction time is 2 h, the catalytic effect is the best, the formaldehyde is completely converted, and the selectivity to hydroxyvaleraldehyde is as high as 98%.

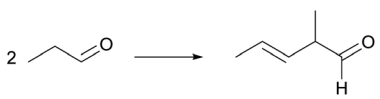

Fig. 19 Self-condensation reaction of propionaldehyde.

Sang-Hyun Pyo[71] used strong basic anion exchange resin IRA-401 with quaternary amine group to catalyze the self-condensation reaction of propionaldehyde. The reaction route is shown in Fig. 19. When the reaction time was 1 h, the reaction temperature was 35 °C, and the amount of IRA-401 resin was 14 mol%, the conversion of propionaldehyde in aqueous solution was 97%, and the yield of 2-methyl-2-pentenal was 95%. Tang[72] also studied the self-condensation reaction of propionaldehyde. He also used anion exchange resin and toluene as solvent, but the yield of 2-methyl-2-pentenal was lower than that of Sang-Hyun Pyo *et al.* This may be because IRA-401 is a strong basic anion exchange resin, which can dissociate OH-in water and act as a Brønsted base site, providing a highly hydrophilic environment for propionaldehyde condensation,[73] so the yield is higher.

Dr Werner Bonrath[74] used five basic resins that can produce quaternary ammonium ions, two of which are polystyrene-based resins, namely Amberlyst™ A26-OH and Amberlyst™ 4, and the other three are polypropylene-based resins, namely Amberlyst™ 1, Amberlyst™ 2 and Amberlyst™ 3, to catalyze the aldol condensation reaction between citral and acetone to prepare β-ionone. The reaction route is shown in Fig. 20. When the reaction temperature is 40 °C, the reaction time is 3 h, and the catalyst is Amberlyst™ 4, the highest conversion of citric acid is 95%, and the highest selectivity to β-ionone is 70%. However, during the cycle, the reactivity decreased, which may be due to the production of insoluble compounds, that is, the polycondensation products of acetone and citral, some of which covered the resin pores and active sites. It may also be that when using alkaline ion exchange resin, the reaction temperature is too high, and the Hoffman elimination reaction occurs at the active site.[75] Resin manufacturers such as Amberlyst™ A26-OH recommend that the maximum use temperature of the resin is 60 °C to avoid deactivation. Daniel J. W. Chong[76] used Amberlyst™ A26-OH to catalyze the aldol condensation reaction between citral and 2-octanone. When the molar ratio of 2-octanone to citral was 10 : 1, the amount of catalyst was 5% of the molar amount of citral, the reaction temperature was 60 °C, and the reaction time was 3.5 h, the highest product yield was 93%.

Alkaline catalytic mechanism

Under the catalysis of alkali, the α-H of the carbonyl group is removed to form a carbon anion, and its resonant structure is an enol anion. The group provides a negatively charged carbon system, while the unattacked carbonyl group provides a slightly positively charged system. The formation of a new carbon–carbon bond is completed by the nucleophilic addition of the carbon anion to the carbonyl group.

Alkaline catalysis and the above acidic catalysis face the same problems and challenges in the future, which are no longer conducting a discussion here.

Acid–base amphoteric catalyst

For specific reactions, acid or alkaline catalyst, too strong or too weak, will lead to the reaction target product yield or selectivity

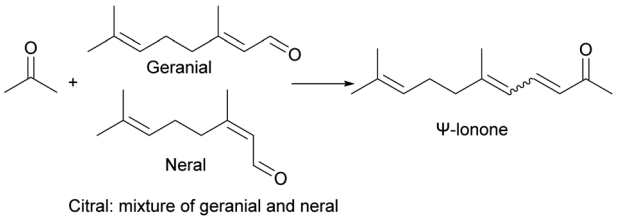

Fig. 20 Condensation reaction of acetone with germanial.

decreased, and acid–base amphoteric catalyst, in theory, can avoid this problem. Ai Mamoru[77] used different oxides as catalysts to study the condensation of formaldehyde and acetaldehyde to acrolein. In the use of acidic oxides, such as MoO_3, WO_3, to obtain the target product acrolein reaction, a higher selectivity, but lower yields. When using alkaline oxides, such as MgO, the target product acrolein has a higher yield but lower selectivity. Therefore, the maximum yield and selectivity can be obtained by adjusting the acid–base ratio in theory. Aleksandra[78] used different acid or alkaline catalysts, such as MgO, Mg–SiO_2, NbP, HPA/SiO_2, *etc.*, to catalyze the cross-aldehyde reaction of formaldehyde and acetaldehyde, and then further dehydrate to prepare acrolein, but this reaction also needs to consider the effect of acetaldehyde self-acetalization reaction. Studies[79–82] have shown that the cross-aldehyde reaction between formaldehyde and acetaldehyde and the self-acetalization reaction of acetaldehyde can be regulated by the acid–base sites of the catalyst. Aleksandra verified that the continuous enhancement of alkalinity will promote the formation of carbon oxides, but the presence of strong base sites is also a necessary condition for increasing the yield of acrolein,[83] while the enhancement of acidity will increase the yield of acrolein and limit the formation of carbon oxides. When the ratio of strong base to strong acid active site is close to 1, the acrolein yield has the maximum value.

Xiao Fang Yu[84] explored the effect of the distance between the acidic and basic sites on the catalyst surface on the aldol condensation reaction activity. Amino acids have –COOH and –NH_2 groups, which can be used to catalyze aldol condensation reaction of *p*-nitrobenzaldehyde and acetone. For example, proline and its derivatives have high activity in catalyzing aldol condensation.[85,86] Xiao Fang Yu immobilized different amino groups of lysine on mesoporous SiO_2 to construct acidic and alkaline sites with different spacing. When the catalyst (Min) with the closest acid–base site is used to catalyze the aldol condensation reaction between 4-nitrobenzaldehyde and acetone, the best result can be obtained, that is, the conversion rate of 4-nitrobenzaldehyde is 90%, and TON is 7.4. This indicates that the synergistic catalysis of the surface depends on the distance between the two functional groups on the surface being close enough to interact with each other or with the reaction molecules. On the contrary, the larger the acid–base site distance, the weaker the interaction, and is not conducive to proton transport. The distance between acid–base sites can be regulated within a certain range, but the interaction between

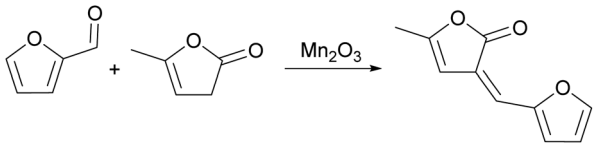

Fig. 21 Condensation reaction of furfural and angelica lactone.

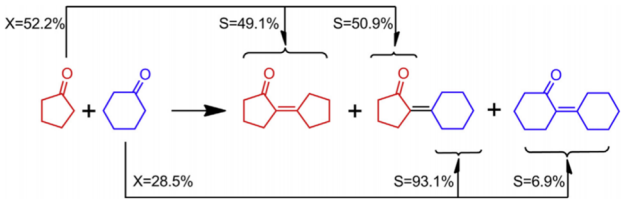

Fig. 22 Condensation reaction of cyclopentanone and cyclohexanone.

acid–base sites cannot be destroyed. This is because the larger the acid–base distance, the smaller the activity of the catalyst.

Ji Lei Xu[87] used Mn_2O_3, an amphoteric metal oxide with low acidity and low alkalinity, as an aldol condensation catalyst. In the article used to catalyze the reaction of furfural and angelica lactone, the reaction route is shown in Fig. 21. When the substrate was 10 mmol, the yield of C_{10} oxide carbon was as high as 96% at 80 °C for 4 h. In most studies of furfural aldol condensation, the polymerization or Cannizzaro reaction of furfural results in a decrease in catalyst activity.[66,88,89] Moreover, furfural polymerization occurs in the presence of strong acid sites. In summary, this is the reason why Mn_2O_3 catalyzed this reaction can achieve excellent results. If we want to further regulate the acid–base ratio, it is necessary to clarify the acid–base effect in the catalyst and the corresponding reaction path.

Mi Wan[90] used ZrO_2 to catalyze the self-condensation and cross-condensation of cyclopentanone and/or cyclohexanone. The reaction route is shown in Fig. 22. The self-condensation reactivity of C5 (49.1%) is higher than that of C6 (6.9%) at 130 °C under atmospheric pressure without solvent. This is because both C5 and C6 are easily adsorbed on the ZrO_2 surface and both have high binding energies. However, the adsorbed C6 has a higher keto–enol isomerization energy barrier, which makes C6 (82 kJ mol^{-1}) less susceptible to activation than C5 (34 kJ mol^{-1}), so the C6 self-condensation reaction activity is low. When cross-condensation was performed, the reaction energy barrier was significantly reduced due to the formation of metastable C7 ring intermediates, so the yield of C_{11} was 50.9%.

Nguyen Thanh[91] used anatase TiO_2 to catalyze the aldol condensation reaction between furfural and acetone. When TiO_2 was not calcined, its activity was comparable to other

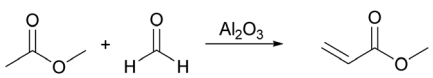

Fig. 23 Condensation reaction of methyl acetate (Ma) and formaldehyde.

catalysts, such as Mg–Al hydrotalcite and BEA zeolite. Only C_8 exists in the reaction product, indicating that the reaction is carried out at an alkaline site. However, the presence of acidic sites can also promote the aldol condensation, that is, to promote product dehydration. These acid–base active sites are distributed on the surface of TiO_2. When TiO_2 is calcined, its catalytic activity will decrease due to a large amount of dehydration and surface dehydroxylation of TiO_2, and high temperature calcination will occur. Anatase to rutile crystal transformation.[92,93]

Qiang Bao[94] used Al_2O_3 with different calcination temperatures to catalyze the aldol condensation reaction between methyl acetate (Ma) and formaldehyde to prepare methyl acrylate (MA). The reaction route is shown in Fig. 23. When the calcination temperature of Al_2O_3 is 500 °C, the reaction temperature is 390 °C, the amount of catalyst is 0.5 mol%, the molar ratio of methyl acetate to formaldehyde is 1 : 2, the feed rate is 0.06 mL min^{-1}, the conversion of methyl acetate is 33.4% and the selectivity of methyl acrylate is 85.8%. The high selectivity of the results is mainly related to the structure of Al_2O_3 itself, its surface contains hydroxyl groups, and Lewis acid sites, in the form of Al atoms, the surface of the O as a basic site.[95,96] When the calcination temperature of Al_2O_3 is higher, the CO_2 adsorption capacity of Al_2O_3 is smaller, which indicates that high temperature calcination will lose some basic sites. Interestingly, as the temperature increases, the selectivity of methyl acrylate decreases, and when the calcination temperature is 1200 °C, which is sufficient to remove the acidic sites on the surface of Al_2O_3 and leave some basic sites, the catalyst is inactive for the cross-condensation reaction between methyl acetate and formaldehyde. This can further explain that the Lewis acid site is dominant in this reaction, and the weak base site is supplemented.

In addition to amphoteric oxides as acid–base amphoteric catalysts, bimetallic catalysts can also be prepared as amphoteric catalysts for catalytic aldol condensation reaction. Yanan Wang[97] loaded lanthanum and cesium on SBA-15 and used it as an acid–base bifunctional catalyst for the aldol condensation reaction between methyl propionate (MP) and formaldehyde (FA) to synthesize methyl methacrylate (MMA). The reaction route is shown in Fig. 24. When the reaction temperature is 350 °C, the molar ratio of MP : FA : methanol is 1 : 1 : 1.5, the specific metal loading Cs and La are 15% and 0.1%, respectively, and when the catalyst calcination temperature is 450 °C, the conversion of MP is 29.2%, and the selectivity of MMA is as high as 90.4%. The conversion rate of MP increased with the increase of Cs loading. When the loading was 15%, the conversion rate tended to be stable.[98] This reaction required the presence of acid–base sites at the same time,[99] in which MP is activated by an alkaline site and formaldehyde by an acidic site, and the reaction intermediates react with each other to form MAA.[100] When La is 0.1%, the catalyst has a higher density of medium basic sites and a lower density of weak acid sites than other catalysts with different La contents. The catalyst acid site is too high will lead to acid–base ratio is not appropriate, resulting in carbon deposition, and the more La content, the easier La aggregation, therefore, the optimal content of La is 0.1%.

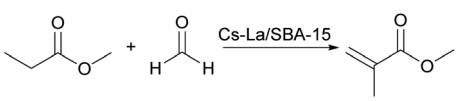

Fig. 24 Condensation reaction of methyl propionate (Ma) and formaldehyde.

According to the self-condensation characteristics of acetone, A. A. Nikolopoulos[101] synthesized hydrotalcite-derived Mg–Al amphoteric oxide supported Pd and Pt catalysts for catalyzing the aldol condensation of acetone itself and hydrogenation to MIBK. The specific reaction route is shown in Fig. 25. Diacetone alcohol (DAA, 4-hydroxy-4-methyl-2-pentanone) was synthesized by self-condensation of acetone. In the second step, DAA was dehydrated to form 4-methyl-3-pentanone (MO). Finally, the carbon–carbon double bond of MO was selectively hydrogenated to form MIBK. The catalytic generation of DAA requires the catalysis of acidic or basic sites, while the dehydration of DAA to MO requires the catalysis of acidic sites, and the selective hydrogenation of MO to MIBK requires the catalysis of metal sites.[102–104] Therefore, the reaction is prone to excessive condensation, or non-selective hydrogenation to form by-products. Based on this, the reaction catalyst is Pd 0.1wt%/HT, which is due to the yield of MIBK is directly related to the alkalinity of the supported metal. When the reaction temperature is 130 °C, the pressure of 0.25% H_2-0.75% N_2 is 400 psi, and the reaction time is 5 h, the conversion of acetone is 38%, but MIBK has a high selectivity of 82.2%.

Acid–base amphoteric catalytic mechanism

Under acid–base catalysis, it belongs to the competition problem of catalytic mechanism, so it is related to the acid–base performance of the catalyst prepared by itself. In principle, the hydrogen on the carbon connected to the electron-withdrawing group is active. Under appropriate conditions (generally alkaline), the hydrogen is removed in the form of positive ions, and a negatively charged carbon system is generated. The nucleophilic addition of carbonyl groups of aldehydes and ketones to form new carbon–carbon bonds.

The difference between acidic, alkaline or acid–base amphoteric catalysts in the aldol condensation reaction is that the structure of each reaction substrate is different, the

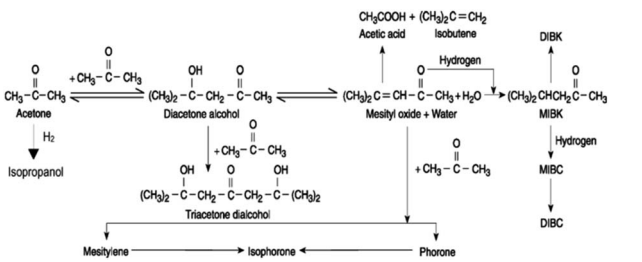

Fig. 25 Main reaction pathways in the acetone condensation process.

structure determines the nature, and the nature determines the reaction mode, which leads to aldol condensation reactions. Strong base or weak base catalysis, which requires specific analysis of specific issues. It can be seen from the article that the yield of C8 is 30.6% when acidic molecular sieve is used in the aldol condensation reaction between furfural and acetone, and its catalytic performance is related to the structure and pore size of molecular sieve. When the solid base Mg–Zr was used to catalyze the reaction, the yield of C13 was 60%. When the strong solid base MgO–ZrO_2 was used to catalyze the reaction, the yield of C13 was about 85%. When the heterogeneous catalyst was replaced by the homogeneous catalyst NaOH, the yield of C13 could reach 97.4%. The selection criteria of these catalysts in the specific reaction, for the aldol condensation reaction, first of all to produce a negatively charged carbon system, based on this phenomenon, letting the original system leave the positively charged ions, so the alkaline catalyst is the first choice, followed by acidity. However, for a complex reaction, the reaction process often includes multiple bond breaking processes, so multiple active centers are required. Sometimes a single catalyst can meet this demand, but more often, multiple catalysts may be needed to achieve selective catalysis. For example, when TiO_2 is used to catalyze the aldol condensation reaction between furfural and acetone, the yield of the catalyst without calcination before use is greater than that of the catalyst with calcination before use, which is the presence of acidic and alkaline sites on its surface. This is due to the dehydration of high temperature calcination, which reduces the acid sites of the system. Therefore, for a single catalyst, it can only play a role in activating a certain step in the reaction, but if the catalyst is compounded that is an acid–base amphoteric catalyst in this paper, and the reaction can be achieved to obtain the target product.

Ionic liquids

Lijun Zhang[105] used lanthanide metal ionic liquid $[(Me_3Si)_2N]_3Ln(\mu\text{-}Cl)Li(THF)_3$ as catalyst to catalyze the aldol condensation reaction between aromatic aldehydes and cyclic ketones under microwave irradiation. The maximum yield of α,α′-bis (substituted benzylidene)cycloalkanones was 91% when the reaction substrate was benzaldehyde and cyclohexanone, the molar ratio of aldehyde to ketone was 2 : 1, the microwave irradiation was 300 W, the reaction time was 6 min, and the amount of ionic liquid was 0.1 mol%. Based on this experimental phenomenon and the existing mechanism, that is, the coordination ability of ketone to lanthanide central metal is stronger than that of aldehyde, in other words, ketone may form a stable complex[106] with lanthanide ion + Lewis acid. It can be considered that the reaction mechanism of aldol condensation catalyzed by this catalyst, namely $[(Me_3Si)_2N]_3Ln\text{-}(\mu\text{-}Cl)Li(THF)_3$, involves the same effect between Ln^{3+} and Li^+ cations.

Chenjie Zhu[107] used ionic liquid $[H_3N^+\text{–}CH_2\text{–}CH_2\text{–}OH][CH_3COO^-]$ (EAIL) as catalyst to catalyze the aldol condensation reaction between acetoin and furfural. When the reaction temperature is 50 °C, the molar ratio of acetoin to 5-methylfurfural (5-MF) is 1 : 1, the solvent is water (15 mL), and the amount of EAIL is 1.5 mol%, 4-hydroxy-1-(5-methylfuran-2-yl) pent-1-en-3-one (2d) has a maximum yield of about 87%, which can be further improved. In the chromatographic test results, unknown polymers were formed, which may be due to the low stability of 5-MF under alkaline water conditions. The configuration of ionic liquids can be used to prepare task-specific ionic liquids (TSILs)[108] for specific reactions, thereby improving the reaction yield.

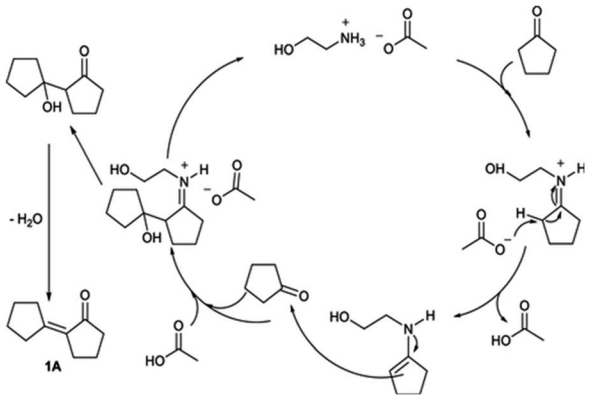

Fig. 26 Self-aldol condensation of cyclopentanone.

Ran Wang[109] used ionic liquid ethanolamine acetic acid (EAOAc) as a catalyst to catalyze the aldol condensation reaction of cyclopentanone itself. The reaction route is shown in Fig. 26.

When the reaction temperature was 100 °C, the reaction time was 6 h, and the molar ratio of reactant to catalyst was 10 : 1.5, the maximum yield of [1,1′-bi(cyclopentylidene)]-2-one was 83.5%. Interestingly, when the reaction was catalyzed by ethanolamine (EA) and acetic acid (HOAc), respectively, the yield of [1,1′-bi(cyclopentylidene)]-2-one was greatly reduced. It can be inferred that there is a synergistic effect between EA and HOAc.

Other catalyst

Ran Wang[110] used $Zn_3Mo_2O_9$ as a catalyst to catalyze the intramolecular aldol condensation of 2,5-hexanedione (HD) and then generate methylcyclopentadiene (MCPD) by selective hydrodeoxygenation. The reaction route is shown in Fig. 27. When the reaction temperature is 400 °C, the hydrogen pressure is 0.1 MPa, WHSV = 2.86 g h^{-1}, and the molar ratio of hydrogen to HD is 67.7, MCPD has a maximum yield of about 65%. When the catalyst has acidic sites, it will inevitably lead to the dehydration of HD to 2,5-dimethylfuran (DMF), and the intramolecular aldol condensation of HD requires alkali catalysis. This view can be proved by the fact that the yield of MCP from intramolecular aldol condensation of HD catalyzed by ZnO or zinc molybdate is about 95%.

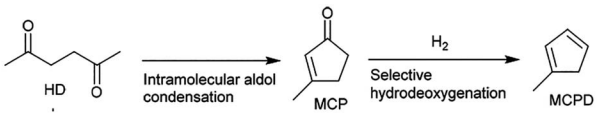

Fig. 27 Intramolecular aldol condensation of 2,5-hexanedione.

Conclusions and outlook

Aldol condensation reaction is a method to form C–C bond and reduce the O/C ratio in the molecule. Growth of carbon chain or intramolecular ring formation β-hydroxyaldehydes or ketones, or α,β-unsaturated aldehydes and ketones. In summary, acidic catalyst, alkaline catalyst, acid–base amphoteric catalyst, ionic liquid and other catalyst can catalyze the aldol condensation reaction. The catalytic performance of acidic resin is weaker than that of EDS when catalyzing the aldol condensation reaction between furfural and cyclopentanone. The yield of acid catalyst for the reaction of furfural and ketone is not high, because furfural is easy to decompose under acid catalyst to produce humin, which is covered on the surface of catalyst and loses its activity. Higher yields can also be obtained for those without furfural. When catalyzing the aldol condensation reaction between furfural and acetone by different catalysts, the catalytic performance of the catalyst is as follows: acidic molecular sieve < solid base < strong solid base < liquid base. While the traditional aldol condensation catalyst, homogeneous alkaline catalyst is more commonly used, but it is not easy to separate and purify. Therefore, the research focus has been shifted to heterogeneous alkaline catalyst research, which reduces the corrosion of the reactor and facilitates the separation of the product. On this basis, the heterogeneous amphoteric catalyst with acid–base properties can not only retain the advantages of heterogeneous acidity or alkalinity, namely reducing the corrosion of the vessel and the easy separation of the product, but also have the characteristics of high selectivity and high activity for the aldol condensation reaction. This is the result of the regulation of the acidic or alkaline active sites on the catalyst surface, and it is also an important direction for the development of the aldol condensation reaction catalyst. Ionic liquid catalyst has the advantages of high activity, strong catalytic effect, good stability, strong applicability of raw materials and low production cost.

Aldol condensation of biomass platform compound can be carried out in acidic catalysts, basic catalysts, acid–base amphoteric catalysts, ionic liquids and other catalyst. The catalytic performance of catalysts between different reactions in the different category requires specific analysis of specific issues. When selecting the reaction catalyst, the specific scheme for preparing the catalyst can be determined according to the size of the substrate molecule, the spatial structure, the acid–base strength of the catalyst itself, and the size of the pore structure. From the listed data in this paper, the basic catalyst has good catalytic activity, while the basic resin has good catalytic activity, low reaction temperature, and is easy to separate from the target product. In the future, the development of strong alkaline resin is a good research direction in the application of aldol condensation of biomass derivatives.

Author contributions

X. Zhang, Y. Li, C. Qian, L. An, X. Li, X. Zhao and Z. Li collected relevant information. X. Zhang and W. Wang co-wrote the paper. All the authors discussed the results and provided input for the manuscript.

Conflicts of interest

There are no conflicts to declare.

Acknowledgements

This work was supported by Key Scientific Research Plan of Shaanxi Provincial Education Department in 2020 (20JS013), and Shaanxi Natural Science Basic Research Program (S2020-JC-WT-0001 and 2020JM-598) and the Open Project of Shaanxi Key Laboratory of Catalysis (SLGPT2019KF01-24).

Notes and references

1 G. W. Huber, S. Iborra and A. Corma, *Chem. Rev.*, 2006, **106**, 4044–4098.
2 A. Corma, O. de la Torre and M. Renz, *Energy Environ. Sci.*, 2012, **5**, 6328–6344.
3 Y. Liu, G. Li, Y. Hu, A. Wang, F. Lu, J.-J. Zou, Y. Cong, N. Li and T. Zhang, *Joule*, 2019, **3**, 1028–1036.
4 A. Bohre, M. I. Alam, K. Avasthi, F. Ruiz-Zepeda and B. Likozar, *Appl. Catal., B*, 2020, **276**, 119069.
5 S. Li, N. Li, G. Li, L. Li, A. Wang, Y. Cong, X. Wang, G. Xu and T. Zhang, *Appl. Catal., B*, 2015, **170–171**, 124–134.
6 Y.-B. Huang, Z. Yang, J.-J. Dai, Q.-X. Guo and Y. Fu, *RSC Adv.*, 2012, **2**, 11211–11214.
7 Y. Jing, Q. Xia, J. Xie, X. Liu, Y. Guo, J.-j. Zou and Y. Wang, *ACS Catal.*, 2018, **8**, 3280–3285.
8 X. Luo, R. Lu, X. Si, H. Jiang, Q. Shi, H. Ma, C. Zhang, J. Xu and F. Lu, *J. Energy Chem.*, 2022, **69**, 231–236.
9 C. Liu, Y. Hu, G. Li, A. Wang, Y. Cong, X. Wang, T. Zhang and N. Li, *Sustainable Energy Fuels*, 2022, **6**, 834–840.
10 J. He, Q. Qiang, S. Liu, K. Song, X. Zhou, J. Guo, B. Zhang and C. Li, *Fuel*, 2021, **306**, 121765.
11 A. A. Timothy, F. Han, G. Li, J. Xu, A. Wang, Y. Cong and N. Li, *Sustainable Energy Fuels*, 2020, **4**, 5560–5567.
12 H. Poole, J. Gauthier, J. R. Vanderveen, P. G. Jessop and R. Lee, *Green Chem.*, 2019, **21**, 6263–6267.
13 T. Moteki, A. T. Rowley and D. W. Flaherty, *ACS Catal.*, 2016, **6**, 7278–7282.
14 Y. Liu, Y. Wang, Y. Cao, X. Chen, Q. Yu, Z. Wang and Z. Yuan, *ACS Sustainable Chem. Eng.*, 2020, **8**, 6949–6955.
15 W. Wang, X. Ji, H. Ge, Z. Li, G. Tian, X. Shao and Q. Zhang, *RSC Adv.*, 2017, **7**, 16901–16907.
16 T. Seki, J.-D. Grunwaldt and A. Baiker, *Chem. Commun.*, 2007, 3562–3564, DOI: **10.1039/B710129E**.
17 W.-B. Yi and C. Cai, *J. Fluorine Chem.*, 2008, **129**, 524–528.
18 O. Kikhtyanin, V. Kelbichová, D. Vitvarová, M. Kubů and D. Kubička, *Catal. Today*, 2014, **227**, 154–162.
19 A. Al-Ani, C. Freitas and V. Zholobenko, *Microporous Mesoporous Mater.*, 2020, **293**, 109805.
20 D. Zhai, Y. Liu, H. Zheng, L. Zhao, J. Gao, C. Xu and B. Shen, *J. Catal.*, 2017, **352**, 627–637.
21 Y. Jing, Y. Xin, Y. Guo, X. Liu and Y. Wang, *Chin. J. Catal.*, 2019, **40**, 1168–1177.
22 Q.-N. Xia, Q. Cuan, X.-H. Liu, X.-Q. Gong, G.-Z. Lu and Y.-Q. Wang, *Angew. Chem., Int. Ed.*, 2014, **53**, 9755–9760.

23 A. S. Amarasekara, B. Wiredu, T. L. Grady, R. G. Obregon and D. Margetić, *Catal. Commun.*, 2019, **124**, 6–11.
24 J. D. Lewis, S. Van de Vyver and Y. Roman-Leshkov, *Angew. Chem., Int. Ed.*, 2015, **54**, 9835–9838.
25 A. Corma, L. T. Nemeth, M. Renz and S. Valencia, *Nature*, 2001, **412**, 423–425.
26 L. Bui, H. Luo, W. R. Gunther and Y. Román-Leshkov, *Angew. Chem., Int. Ed.*, 2013, **52**, 8022–8025.
27 M. Moliner, Y. Román-Leshkov and M. E. Davis, *Proc. Natl. Acad. Sci. U. S. A.*, 2010, **107**, 6164–6168.
28 G. Nie, J.-J. Zou, R. Feng, X. Zhang and L. Wang, *Catal. Today*, 2014, **234**, 271–277.
29 M. Boronat, A. Corma and M. Renz, *J. Phys. Chem. B*, 2006, **110**, 21168–21174.
30 H. Y. Luo, D. F. Consoli, W. R. Gunther and Y. Román-Leshkov, *J. Catal.*, 2014, **320**, 198–207.
31 W. Li, M. Su, T. Zhang, Q. Ma and W. Fan, *Fuel*, 2019, **237**, 1281–1290.
32 M. Su, W. Li, T. Zhang, H. Xin, S. Li, W. Fan and L. Ma, *Catal. Sci. Technol.*, 2017, **7**, 3555–3561.
33 W. Dai, S. Zhang, Z. Yu, T. Yan, G. Wu, N. Guan and L. Li, *ACS Catal.*, 2017, **7**, 3703–3706.
34 T. Yan, W. Dai, G. Wu, S. Lang, M. Hunger, N. Guan and L. Li, *ACS Catal.*, 2018, **8**, 2760–2773.
35 T. Yan, S. Yao, W. Dai, G. Wu, N. Guan and L. Li, *Chin. J. Catal.*, 2021, **42**, 595–605.
36 C. R. Ho, S. Zheng, S. Shylesh and A. T. Bell, *J. Catal.*, 2018, **365**, 174–183.
37 S. Wang, K. Goulas and E. Iglesia, *J. Catal.*, 2016, **340**, 302–320.
38 M. Y. Talanova, V. A. Yarchak and E. A. Karakhanov, *Russ. J. Appl. Chem.*, 2019, **92**, 857–864.
39 J. Tian, L. Chen, D.-W. Zhang, Y. Liu and Z.-T. Li, *Chem. Commun.*, 2016, **52**, 6351–6362.
40 E. Merino, E. Verde-Sesto, E. M. Maya, A. Corma, M. Iglesias and F. Sánchez, *Appl. Catal., A*, 2014, **469**, 206–212.
41 J. Fritsch, F. Drache, G. Nickerl, W. Böhlmann and S. Kaskel, *Microporous Mesoporous Mater.*, 2013, **172**, 167–173.
42 M. P. Boronoev, E. S. Subbotina, A. A. Kurmaeva, Y. S. Kardasheva, A. L. Maksimov and E. A. Karakhanov, *Pet. Chem.*, 2016, **56**, 109–120.
43 A. L. Maksimov, E. A. Karakhanov, L. A. Kulikov and M. V. Terenina, *Pet. Chem.*, 2017, **57**, 589–594.
44 H. Gao, F. Han, G. Li, A. Wang, Y. Cong, Z. Li, W. Wang and N. Li, *Sustainable Energy Fuels*, 2022, **6**, 1616–1624.
45 W. Wang, Y. Liu, N. Li, G. Li, W. Wang, A. Wang, X. Wang and T. Zhang, *Sci. Rep.*, 2017, **7**, 6111.
46 M. Gu, Q. Xia, X. Liu, Y. Guo and Y. Wang, *ChemSusChem*, 2017, **10**, 4102–4108.
47 I. Cota, F. Medina, J. E. Sueiras and D. Tichit, *Tetrahedron Lett.*, 2011, **52**, 385–387.
48 J. Yang, N. Li, G. Li, W. Wang, A. Wang, X. Wang, Y. Cong and T. Zhang, *ChemSusChem*, 2013, **6**, 1149–1152.
49 G. Li, N. Li, J. Yang, L. Li, A. Wang, X. Wang, Y. Cong and T. Zhang, *Green Chem.*, 2014, **16**, 594–599.
50 R. Xing, A. V. Subrahmanyam, H. Olcay, W. Qi, G. P. van Walsum, H. Pendse and G. W. Huber, *Green Chem.*, 2010, **12**, 1933–1946.
51 L. Faba, E. Díaz and S. Ordóñez, *Appl. Catal., B*, 2012, **113–114**, 201–211.
52 Y. Li, S. Lian, D. Tong, R. Song, W. Yang, Y. Fan, R. Qing and C. Hu, *Appl. Energy*, 2011, **88**, 3313–3317.
53 M. L. Rojas-Cervantes, L. Alonso, J. Díaz-Terán, A. J. López-Peinado, R. M. Martín-Aranda and V. Gómez-Serrano, *Carbon*, 2004, **42**, 1575–1582.
54 J. Yang, S. Li, N. Li, W. Wang, A. Wang, T. Zhang, Y. Cong, X. Wang and G. W. Huber, *Ind. Eng. Chem. Res.*, 2015, **54**, 11825–11837.
55 S. Feng, X. Zhang, Q. Zhang, Y. Liang, X. Zhao, C. Wang and L. Ma, *Fuel*, 2021, **299**, 120889.
56 O. Kikhtyanin, D. Kadlec, R. Velvarská and D. Kubička, *ChemCatChem*, 2018, **10**, 1464–1475.
57 X. Zhao, S. Li, Y. Hu, X. Zhang, L. Chen, C. Wang, L. Ma and Q. Zhang, *Chem. Eng. J.*, 2022, **428**, 131368.
58 C. Liu, M. Wei, J. Wang, J. Xu, J. Jiang and K. Wang, *ACS Sustainable Chem. Eng.*, 2020, **8**, 5776–5786.
59 P. Domínguez de María, P. Bracco, L. F. Castelhano and G. Bargeman, *ACS Catal.*, 2011, **1**, 70–75.
60 F. Chen, N. Li, S. Li, J. Yang, F. Liu, W. Wang, A. Wang, Y. Cong, X. Wang and T. Zhang, *Catal. Commun.*, 2015, **59**, 229–232.
61 B. Pholjaroen, N. Li, J. Yang, G. Li, W. Wang, A. Wang, Y. Cong, X. Wang and T. Zhang, *Ind. Eng. Chem. Res.*, 2014, **53**, 13618–13625.
62 G. Liang, A. Wang, X. Zhao, N. Lei and T. Zhang, *Green Chem.*, 2016, **18**, 3430–3438.
63 Y. Iwakura and K. Hayashi, *Macromol. Chem. Phys.*, 1960, **36**, 178–189.
64 W. Shen, G. A. Tompsett, K. D. Hammond, R. Xing, F. Dogan, C. P. Grey, W. C. Conner, S. M. Auerbach and G. W. Huber, *Appl. Catal., A*, 2011, **392**, 57–68.
65 E. Ketabchi, L. Pastor-Pérez, T. R. Reina and H. Arellano-García, *Renewable Energy*, 2020, **156**, 1065–1075.
66 C. J. Barrett, J. N. Chheda, G. W. Huber and J. A. Dumesic, *Appl. Catal., B*, 2006, **66**, 111–118.
67 M. A. Tike, A. M. Gharde and V. V. Mahajani, *Asia-Pac. J. Chem. Eng.*, 2008, **3**, 333–346.
68 R. Mahrwald, *Curr. Org. Chem.*, 2003, **7**, 1713–1723.
69 M. Miyagawa and T. Akiyama, *Chem. Lett.*, 2017, **47**, 78–81.
70 T. Seki, H. Tachikawa, T. Yamada and H. Hattori, *J. Catal.*, 2003, **217**, 117–126.
71 S.-H. Pyo, M. Hedström, S. Lundmark, N. Rehnberg and R. Hatti-Kaul, *Org. Process Res. Dev.*, 2011, **15**, 631–637.
72 S. P. Tang, Q. H. Li and D. L. Yin, *J. Nat. Sci. Hunan Norm. Univ.*, 2001, **24**, 42–44.
73 K. Ebitani, K. Motokura, K. Mori, T. Mizugaki and K. Kaneda, *J. Org. Chem.*, 2006, **71**, 5440–5447.
74 W. Bonrath, Y. Pressel, J. Schütz, E. Ferfecki and K.-D. Topp, *ChemCatChem*, 2016, **8**, 3584–3591.
75 D. V. Banthorpe, E. D. Hughes and C. Ingold, *J. Chem. Soc.*, 1960, 4054–4087, DOI: **10.1039/JR9600004054**.

76 D. J. W. Chong, F. H. L. Chong and J. Latip, *Green Process. Synth.*, 2016, **5**, 297–304.
77 M. Ai, *Bull. Chem. Soc. Jpn.*, 1991, **64**, 1346–1350.
78 A. Lilic, T. T. Wei, S. Bennici, J. F. Devaux, J. L. Dubois and A. Auroux, *Chemsuschem*, 2017, **10**, 3459–3472.
79 C. Cobzaru, S. Oprea, E. Dumitriu and V. Hulea, *Appl. Catal., A*, 2008, **351**, 253–258.
80 E. Dumitriu, C. Cobzaru, V. Hulea and S. Oprea, *Rev. Chim.*, 2010, **61**, 400–403.
81 A. Azzouz, D. Messad, D. Nistor, C. Catrinescu, A. Zvolinschi and S. Asaftei, *Appl. Catal., A*, 2003, **241**, 1–13.
82 E. Dumitriu, V. Hulea, I. Fechete, A. Auroux, J. F. Lacaze and C. Guimon, *Microporous Mesoporous Mater.*, 2001, **43**, 341–359.
83 A. Lilic, S. Bennici, J. F. Devaux, J. L. Dubois and A. Auroux, *Chemsuschem*, 2017, **10**, 1916–1930.
84 X. Yu, X. Yu, S. Wu, B. Liu, H. Liu, J. Guan and Q. Kan, *J. Solid State Chem.*, 2011, **184**, 289–295.
85 E. G. Doyagüez, F. Calderón, F. Sánchez and A. Fernández-Mayoralas, *J. Org. Chem.*, 2007, **72**, 9353–9356.
86 G. Yang, Z. Yang, L. Zhou, R. Zhu and C. Liu, *J. Mol. Catal. A: Chem.*, 2010, **316**, 112–117.
87 J. Xu, N. Li, X. Yang, G. Li, A. Wang, Y. Cong, X. Wang and T. Zhang, *ACS Catal.*, 2017, **7**, 5880–5886.
88 L. Hora, V. Kelbichová, O. Kikhtyanin, O. Bortnovskiy and D. Kubička, *Catal. Today*, 2014, **223**, 138–147.
89 O. Kikhtyanin, D. Kubička and J. Čejka, *Catal. Today*, 2015, **243**, 158–162.
90 M. Wan, D. Liang, L. Wang, X. Zhang, D. Yang and G. Li, *J. Catal.*, 2018, **361**, 186–192.
91 D. Nguyen Thanh, O. Kikhtyanin, R. Ramos, M. Kothari, P. Ulbrich, T. Munshi and D. Kubička, *Catal. Today*, 2016, **277**, 97–107.
92 N. Wetchakun and S. Phanichphant, *Curr. Appl. Phys.*, 2008, **8**, 343–346.
93 M. E. Simonsen and E. G. Søgaard, *J. Sol-Gel Sci. Technol.*, 2010, **53**, 485–497.
94 Q. Bao, T. Bu, J. Yan, C. Zhang, C. Ning, Y. Zhang, M. Hao, W. Zhang and Z. Wang, *Catal. Lett.*, 2017, **147**, 1540–1550.
95 X. Liu and R. E. Truitt, *J. Am. Chem. Soc.*, 1997, **119**, 9856–9860.
96 C. Morterra and G. Magnacca, *Catal. Today*, 1996, **27**, 497–532.
97 Y. Wang, R. Yan, Z. Lv, H. Wang, L. Wang, Z. Li and S. Zhang, *Catal. Lett.*, 2016, **146**, 1808–1818.
98 B. Li, R. Yan, L. Wang, Y. Diao, Z. Li and S. Zhang, *Catal. Lett.*, 2013, **143**, 829–838.
99 J. J. Spivey, M. R. Gogate, J. R. Zoeller and R. D. Colberg, *Ind. Eng. Chem. Res.*, 1997, **36**, 4600–4608.
100 M. R. Gogate, J. J. Spivey and J. R. Zoeller, *Catal. Today*, 1997, **36**, 243–254.
101 A. A. Nikolopoulos, B. W. L. Jang and J. J. Spivey, *Appl. Catal., A*, 2005, **296**, 128–136.
102 Y. Higashio and T. Nakayama, *Catal. Today*, 1996, **28**, 127–131.
103 N. N. Das and S. C. Srivastava, *Bull. Mater. Sci.*, 2002, **25**, 283–289.
104 Y. Onoue, Y. Mizutani, S. Akiyama, Y. Izumi, Y. Watanabe and J. Maekawa, *Bull. Jpn. Pet. Inst.*, 1974, **16**, 55–59.
105 L. J. Zhang, S. W. Wang, E. H. Sheng and S. L. Zhou, *Green Chem.*, 2005, **7**, 683–686.
106 N. Yoshikawa, Y. M. A. Yamada, J. Das, H. Sasai and M. Shibasaki, *J. Am. Chem. Soc.*, 1999, **121**, 4168–4178.
107 C. Zhu, T. Shen, D. Liu, J. Wu, Y. Chen, L. Wang, K. Guo, H. Ying and P. Ouyang, *Green Chem.*, 2016, **18**, 2165–2174.
108 J. H. Davis Jr, *Chem. Lett.*, 2004, **33**, 1072–1077.
109 R. Wang, G. Li, H. Tang, A. Wang, G. Xu, Y. Cong, X. Wang, T. Zhang and N. Li, *ACS Sustainable Chem. Eng.*, 2019, **7**, 17354–17361.
110 R. Wang, Y. Liu, G. Li, A. Wang, X. Wang, Y. Cong, T. Zhang and N. Li, *ACS Catal.*, 2021, **11**, 4810–4820.